



HAL
open science

Meiosis occurs normally in the fetal ovary of mice lacking all retinoic acid receptors

Nadège Vernet, Diana Condrea, Chloé Mayere, Betty Féret, Muriel Klopfenstein, William Magnant, Violaine Alunni, Marius Telentin, Sirine Souali-Crespo, Serge Nef, et al.

► **To cite this version:**

Nadège Vernet, Diana Condrea, Chloé Mayere, Betty Féret, Muriel Klopfenstein, et al.. Meiosis occurs normally in the fetal ovary of mice lacking all retinoic acid receptors. *Science Advances*, 2020, 6, pp.eaaz1139. 10.1126/sciadv.aaz1139 . hal-02988715

HAL Id: hal-02988715

<https://hal.science/hal-02988715>

Submitted on 4 Nov 2020

HAL is a multi-disciplinary open access archive for the deposit and dissemination of scientific research documents, whether they are published or not. The documents may come from teaching and research institutions in France or abroad, or from public or private research centers.

L'archive ouverte pluridisciplinaire **HAL**, est destinée au dépôt et à la diffusion de documents scientifiques de niveau recherche, publiés ou non, émanant des établissements d'enseignement et de recherche français ou étrangers, des laboratoires publics ou privés.

DEVELOPMENTAL BIOLOGY

Meiosis occurs normally in the fetal ovary of mice lacking all retinoic acid receptors

Nadège Vernet¹, Diana Condrea¹, Chloé Mayere², Betty Féret¹, Muriel Klopfenstein¹, William Magnant¹, Violaine Alunni³, Marius Telentin^{1,4}, Sirine Souali-Crespo¹, Serge Nef², Manuel Mark^{1,4}, Norbert B. Ghyselinck^{1*}

Gametes are generated through a specialized cell differentiation process, meiosis, which, in ovaries of most mammals, is initiated during fetal life. All-*trans* retinoic acid (ATRA) is considered as the molecular signal triggering meiosis initiation. In the present study, we analyzed female fetuses ubiquitously lacking all ATRA nuclear receptors (RAR), obtained through a tamoxifen-inducible cre recombinase-mediated gene targeting approach. Unexpectedly, mutant oocytes robustly expressed meiotic genes, including the meiotic gatekeeper STRA8. In addition, ovaries from mutant fetuses grafted into adult recipient females yielded offspring bearing null alleles for all *Rar* genes. Thus, our results show that RAR are fully dispensable for meiotic initiation, as well as for the production of functional oocytes. Assuming that the effects of ATRA all rely on RAR, our study goes against the current model according to which meiosis is triggered by endogenous ATRA in the developing ovary. It therefore revives the search for the meiosis-inducing substance.

INTRODUCTION

Mammalian meiosis is a germ cell-specific division process that generates haploid gametes from their diploid precursors, oogonia in the female and spermatogonia in the male. In the mouse, female germ cells enter into meiosis before birth, around embryonic day 13.5 (E13.5). During the same embryonic period, male germ cells stop proliferating and enter the G₀/G₁ phase of the cell cycle, thus becoming mitotically quiescent. Male germ cells resume proliferation at birth and then enter into meiosis starting from postnatal day 8.

To account for the sexual dimorphism in the timing of germ cell differentiation, it was hypothesized, notably from transplantation experiments of germ cells (1), that the decision to enter meiosis is controlled by a meiosis-inducing substance (MIS) or/and by a meiosis-preventing substance (MPS) produced by somatic cells (2). Subsequently, it was proposed that all-*trans* retinoic acid (ATRA) and its degrading enzyme CYP26B1 played key roles in controlling the timing of meiosis initiation in female and male gonads, respectively (3, 4). The concept that ATRA is the MIS was, however, challenged by a genetic study demonstrating that meiosis initiation occurs despite the lack of two major ATRA-synthesizing enzymes (5). The recent finding that a third enzyme, expressed in fetal ovaries and capable of ATRA synthesis, is also involved in meiosis revived the model according to which meiosis entry is triggered by endogenous ATRA in the ovary (6).

ATRA is the active metabolite of retinol (vitamin A). Inside cells, conversion of retinol to ATRA depends on retinaldehyde dehydrogenases (ALDH1A isotypes). Then, ATRA activity is mediated by the nuclear retinoic acid receptors (RARA, RARB, and RARG iso-

types), which are ligand-dependent transcriptional regulators. They usually function in the form of heterodimers with rexinoid receptors to control expression of ATRA-target genes, in which they are bound to specific DNA sites called retinoic acid response elements (RARE). In addition, RAR are capable of nongenomic activation events at the cell membrane, similarly to steroid nuclear receptors (7).

As all ATRA-dependent events rely in some way on RAR, we decided to tackle the potential contribution of endogenous ATRA to meiosis in female germ cells by generating and analyzing mice lacking all RAR isotypes. Against the currently admitted model (8, 9), our study reveals that RARs (and therefore endogenous ATRA) are in fact fully dispensable for meiosis in the mouse fetal ovary.

RESULTS

Time course of meiosis and expression of RARs in the fetal ovary

To assess whether the kinetics of primordial germ cell (PGC) migration and timing of meiosis initiation were not modified by either the mixed genetic background or the tamoxifen (TAM) treatments, we determined the expression patterns of POU5F1, as a marker of PGC, and STRA8, as a marker of meiosis initiation, between E11.0 and E14.5 in control fetuses (i.e., TAM-treated *Rara*^{L2/L2}; *Rarg*^{L2/L2}; *Rarb*^{L-/L-} females; see Material and Methods). At E11.0, PGC were specifically observed in the mesentery of the hindgut (white arrow in fig. S1A) and in the undifferentiated gonad (white arrow in fig. S1C), as expected at this developmental stage (10). At E12.5, *Stra8* mRNA were expressed at low levels, but STRA8 protein was undetectable on serial histological sections throughout the ovary (fig. S1, D and G). At E13.5, *Stra8* mRNA were expressed throughout the ovary, but germ cells expressing STRA8 protein were scarce (fig. S1, E and H). At E14.5, numerous germ cells expressed *Stra8* mRNA and/or STRA8 protein (fig. S1, F and I). This expression of STRA8 in developing ovaries of control fetuses treated with TAM is similar, if not identical, to that previously observed in untreated wild-type females (11).

The expression of *Rars* in the fetal gonads is poorly documented. To determine which RAR isotypes are actually present in the ovary,

Copyright © 2020
The Authors, some
rights reserved;
exclusive licensee
American Association
for the Advancement
of Science. No claim to
original U.S. Government
Works. Distributed
under a Creative
Commons Attribution
NonCommercial
License 4.0 (CC BY-NC).

¹Institut de Génétique et de Biologie Moléculaire et Cellulaire (IGBMC), Département de Génétique Fonctionnelle et Cancer, Centre National de la Recherche Scientifique (CNRS UMR7104), Institut National de la Santé et de la Recherche Médicale (INSERM U1258), Université de Strasbourg (UNISTRA), 1 rue Laurent Fries, BP-10142, F-67404 Illkirch Cedex, France. ²Department of Genetic Medicine and Development, University of Geneva Medical School, Geneva, Switzerland. ³GenomEast platform, France Génomique consortium, IGBMC, 1 rue Laurent Fries, F-67404 Illkirch Cedex, France. ⁴Service de Biologie de la Reproduction, Hôpitaux Universitaires de Strasbourg (HUS), France.

*Corresponding author. Email: norbert@igbmc.fr

we performed immunohistochemistry (IHC). At E11.5, RARA was detected in a large number of tissues, including the fetal gonad (Fig. 1, A and C to E). No information was obtained for RARB, since reliable antibodies for RARB are not available (12). RARG was readily detected in cartilages, but not in the ovary (Fig. 1, B and B'). To gain further insights into the expression of *Rars* in germ cells, we took advantage of single-cell RNA sequencing (RNA-seq) experiments performed in CD1 fetuses (13). In female germ cells, *Rara* mRNA expression reached its maximum around E13.5. *Rarb* mRNA levels were always low. The expression of *Rarg* mRNA was highest at E10.5 and then decreased between E11.5 and E12.5 and rose transiently at late E13.5 (Fig. 1F). To verify that the expression of *Rars* was not modified by the mixed genetic background of our fetuses or the TAM treatments, we performed reverse transcription quantitative polymerase chain reaction (RT-qPCR) on single germ cells isolated from control ovaries (i.e., TAM-treated *Rara*^{L2/L2};*Rarg*^{L2/L2};*Rarb*^{L-/L-} females; see above) at E13.5 ($n = 25$) and E14.5 ($n = 40$). Germ cell identity was assigned on the basis of the expression of *Dazl*, *Ddx4*, and *Kit* (Fig. 1G). *Rara* and *Rarg* mRNAs were detected in a majority of germ cells at E13.5 and E14.5 (Fig. 1H), in agreement with the data obtained in CD1 genetic background. No information was obtained for *Rarb* mRNA, since the mice we used were on a *Rarb*-null genetic background. In the end, it is obvious that at least two RAR mRNAs are present in female germ cells with expression levels below the threshold of detection by IHC.

Efficient ablation of all RARs in the developing gonad from E11.5 onward

Given the expression pattern of RARs, we reasoned that full impairment of ATRA signaling in the whole fetal ovary would require the ablation of all three RAR-coding genes. This was not possible by associating *Rara*, *Rarb*, and *Rarg* knockout alleles in a single fetus, because *Rara*^{-/-};*Rarg*^{-/-};*Rarb*^{+/-} embryos do not develop beyond E8.5, precluding analysis of their ovaries (14). To do so, we performed cre/ERT² directed genetic ablation of *Rara* and *Rarg* using a ubiquitously expressed cre/ERT² activated by TAM, before meiotic initiation, but later than E8.5, in the context of a *Rarb*-null background (see Materials and Methods). We first chose to administer TAM at E10.5, shortly after the start of gonad formation, but 3 days before meiosis initiation. Ablation of RARG and RARA was assessed at E11.5, i.e., 24 hours after TAM induction of cre/ERT². Immunostaining for RARG was nearly abolished in mutant embryos in all RARG-expressing tissues (Fig. 2, A to H). Only a few cells reacted with the antibody (arrowheads in Fig. 2), indicating efficient ablation of *Rarg*. Accordingly, Western blot analysis of whole-embryo protein extracts showed almost undetectable levels of RARG in mutant embryos (Fig. 2O). In situ hybridization (ISH) showed that the number of cells expressing *Rara* mRNA was markedly reduced in mutant embryos, including in their gonads where only a few cells still contained single dots (Fig. 2, I to L). In addition, Western blot analysis showed that RARA was undetectable, even with prolonged exposure, in mutant embryos (Fig. 2, O and P). This indicated an efficient loss of RARG and RARA in the whole embryo. At E14.5, the number of cells remaining positive for RARG in mutants was even smaller, while no cell expressed RARA (arrowheads in fig. S2, A to L). Thus, TAM induced an efficient ablation of RARG and RARA, which was almost complete from E11.5 onward.

The pattern of gene excision by cre/ERT² in germ cells was additionally assessed using the *mT/mG* reporter transgene in control and

mutant fetuses (see Materials and Methods). Expression of membrane-targeted green fluorescent protein (mGFP) was detected in all germ cells of the mutants at E11.5 and in almost all of them at E14.5 (fig. S3, A to L). This indicated that cre/ERT²-directed excision of the reporter occurred in almost all germ cells, as early as 24 hours after TAM treatment. In agreement with this finding, *Rara* and *Rarg* mRNAs were not detected in any germ cell isolated from mutant ovaries at E13.5 or E14.5 and analyzed by RT-qPCR (Fig. 1H). These data showed that efficient excision of all RARs occurred in all germ cells.

Ablation of all RARs does not impair meiosis initiation

To investigate the impact of RAR ablation on meiotic initiation, the expression of canonical markers of meiosis was assessed by IHC throughout the anteroposterior axis of the ovary. At E14.5, numerous germ cells in both control and mutant fetuses expressed the synaptonemal protein SYCP3 and the cohesin REC8 (Fig. 3A). The mean number of germ cells and the percentages of SYCP3-positive or REC8-positive germ cells were similar in control and mutant fetuses (Fig. 3, B and C). This indicated that meiosis initiated in germ cells of the mutant fetuses.

To rule out the possibility that the cells that initiated meiosis experienced an inefficient ablation of the RAR-coding genes, we took advantage of the presence of *mT/mG* reporter in the fetuses. The vast majority of the SYCP3- or REC8-positive germ cells of the mutant ovary were mGFP positive (Fig. 4, A to F), indicating excision in almost all meiotic cells. Unexpectedly, mGFP was detected in only few somatic cells of the ovary and the mesonephros, making questionable whether cre/ERT² was efficient or whether the reporter was expressed in these cells. However, mRFP remained expressed in none of them (fig. S3, M to T), indicating that they actually all experienced cre-mediated recombination. To further assess RAR ablation in somatic cells, we performed genomic PCR analysis, using DNA extracted from whole ovaries of E13.5 control and mutant fetuses. Excised (L-), but not conditional (L2), alleles of *Rara* and *Rarg* were detected in genomic DNA isolated from mutant ovaries. In contrast, conditional (L2), but not excised (L-), alleles were always detected in control ovaries (Fig. 4, G and H). Altogether, these data show that efficient excision of all RARs occurs in all of their tissues, including somatic and germ cells in the ovaries.

To further investigate expression of the meiotic program at the cellular level in the absence of RARs, we used RT-qPCR on single cells isolated from ovaries at E13.5 (25 control and 43 mutant germ cells) and E14.5 (40 control and 47 mutant germ cells). Consistent with IHC analyses, the proportion of germ cells expressing *Sycp3* and *Rec8*, as well as their individual levels of expression, were similar in control and mutant ovaries (Fig. 4I). In addition, the cellular expression of 12 other meiosis-specific genes was similar (for *Mei1*, *Meiob*, *Prdm9*, *Stag3*, *Syce1*, *Sycp1*, *Sycp2*, and *Ugt8a*) or slightly but significantly increased (for *Dmcl1*, *Smc1b*, *Spo11*, and *Syce2*) when RAR were absent (fig. S4). This confirmed the commitment of mutant germ cells toward meiosis, despite their lack of RARs.

The meiotic gatekeeper STRA8 (15) was also expressed in germ cells of mutant ovaries, notably in those that underwent cre/ERT²-mediated recombination (Fig. 4, C and F), albeit their number was about half less than that observed in control ovaries (Fig. 3C). Accordingly, *Stra8* mRNA was present in only 30% of the germ cells from mutant ovaries at E13.5 versus 92% in control ovaries. In addition, its expression level was slightly but significantly ($P < 0.001$) decreased when compared with the control situation (Fig. 4I). However, at E14.5,

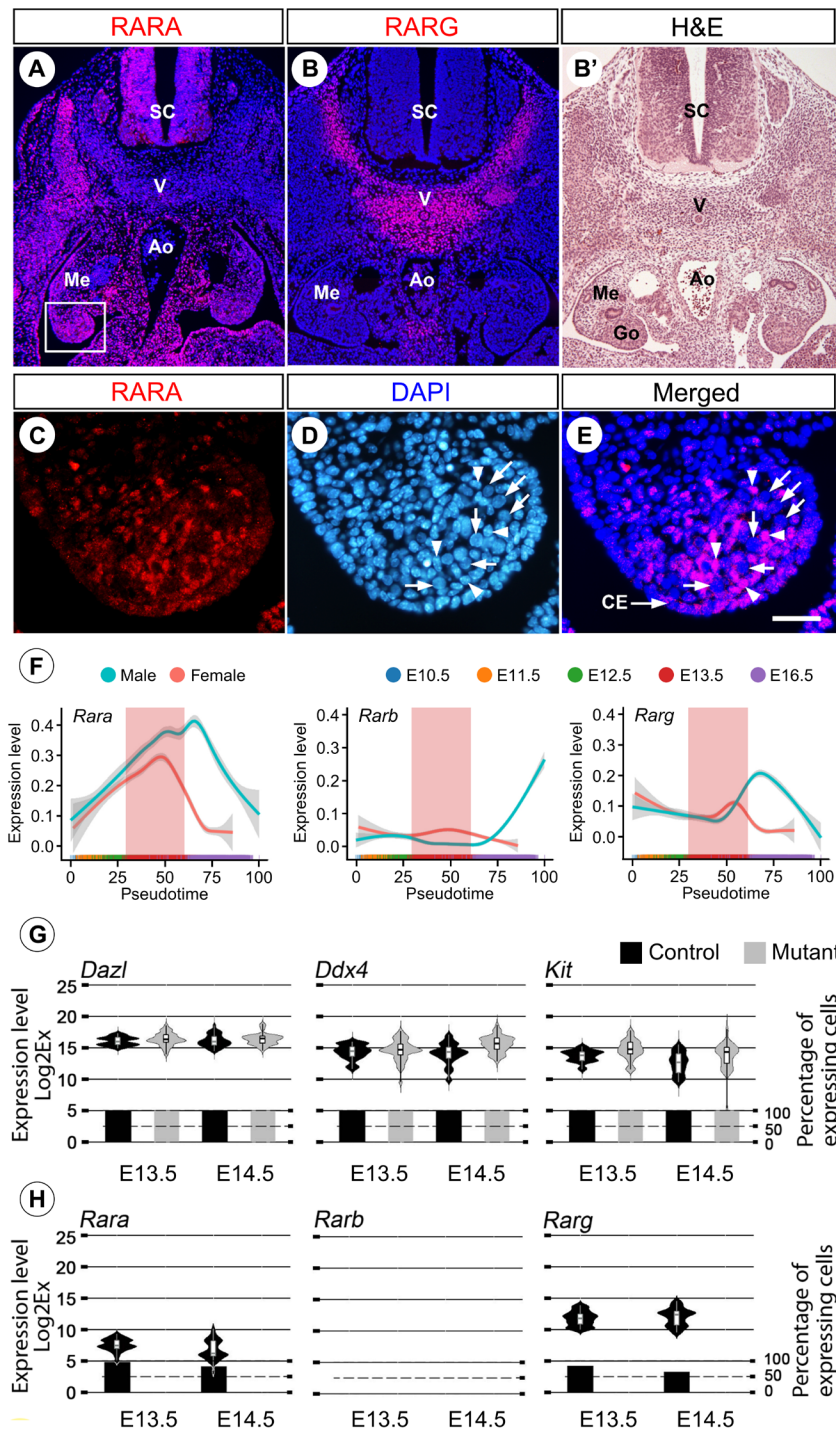


Fig. 1. Expression of RARs in the female gonad and in germ cells during embryonic development. (A and B) Detection of RARA and RARG (red signals) on frontal histological sections of an E11.5 wild-type female embryo: Expression of RARG is confined to the precartilaginous anlage of a vertebra, while that of RARA is more widespread and includes notably the undifferentiated gonad. (B') Same section as (B) stained with H&E. (C to E) Enlargement of the box in (A): RARA (in red) is detected in the nuclei of some somatic cells of the gonad (arrowheads) and of the coelomic epithelium; in contrast, the large, rounded nuclei characteristic of germ cells (arrows) do not exhibit anti-RARA immunostaining. Nuclei are counterstained with DAPI (blue signal). Ao, aorta; CE, coelomic epithelium; Go, gonad; Me, mesonephros; SC, spinal cord; V, vertebra. Scale bar (in E), 160 μ m (A to B') and 30 μ m (C to E). (F) Expression of *Rara*, *Rarb*, and *Rarg* determined by RNA-seq of 14,750 single germ cells isolated from gonads between E10.5 and E16.5. Smoothed expression curves of *Rara*, *Rarb*, and *Rarg* in male (blue lines) and female (pink lines) germ cells ordered by computed pseudotime. The red-shaded boxes indicate the time of meiosis initiation in the fetal ovary. (G and H) RT-qPCR analysis comparing the expression levels and distributions of mRNAs in single germ cells from control and mutant ovaries at E13.5 and E14.5. The violin plot width and length represent, respectively, the number of cells and the range of expression (Log2Ex). The box-and-whisker plots illustrate medians, ranges, and variabilities of the collected data. The histograms show the percentages of expressing cells in each group. Photo credits: Norbert B. Ghyselinck and Manuel Mark, IGBMC.

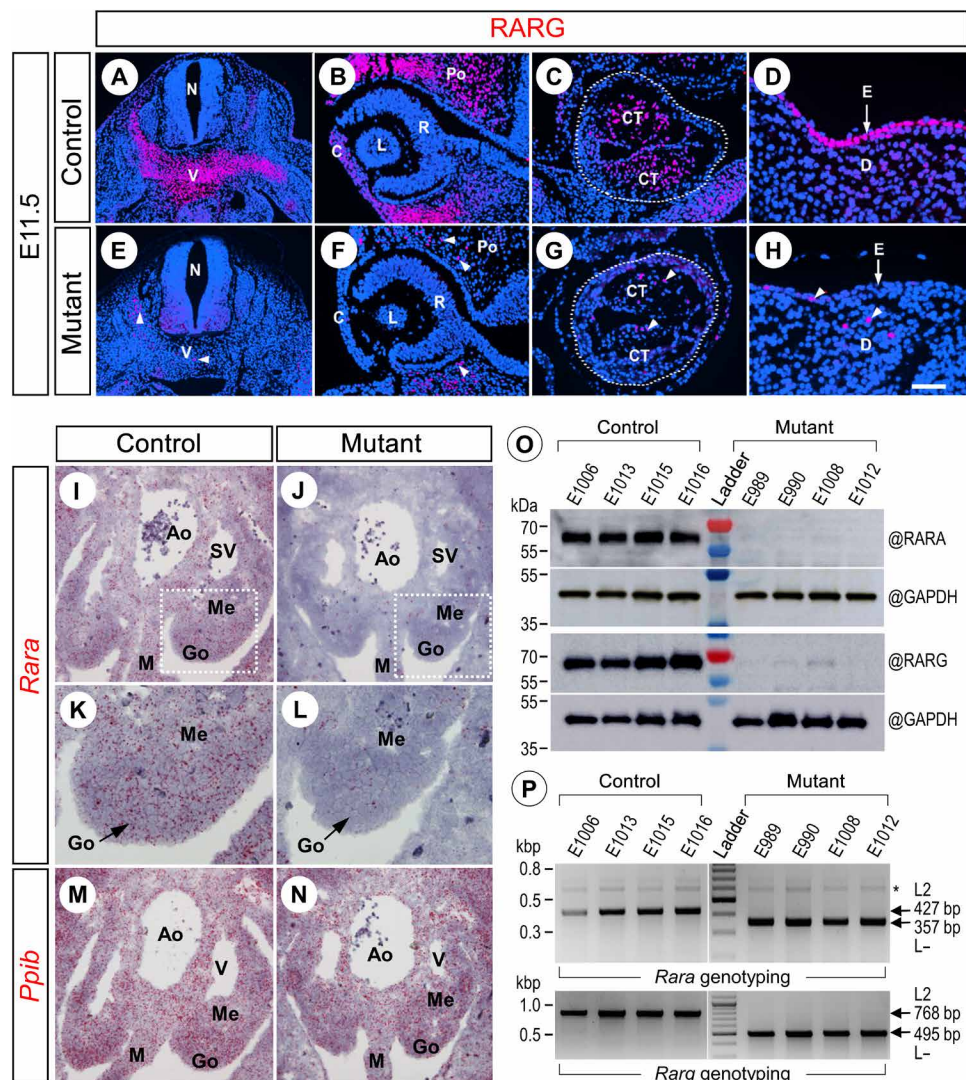


Fig. 2. Excision of RAR after administration of TAM at E10.5. (A to H) Detection of RARG (red signal) on frontal histological sections at similar levels of control and mutant embryos at E11.5, namely, 24 hours after TAM administration. (A to D) RARG is strongly expressed in precartilaginous vertebrae, in periocular and corneal mesenchyme, in conotruncal ridges, and in epidermis of the control embryo. (E to H) Expression of RARG is nearly abolished in the tissues of the mutant embryo. White arrowheads indicate few nuclei that are still expressing RARG in the mutant tissues. Nuclei are counterstained with DAPI (blue signal). (I to L) ISH showing expression of *Rara* mRNA (I to L) and of *Ppib* mRNA (M and N) detected by red color staining in control and mutant embryos at E11.5. Only a few red dots indicative of *Rara* mRNA are observed in the mutant. In contrast, red dots indicative of the ubiquitously expressed *Ppib* mRNA were as numerous in mutant and control embryos. (O) Western blot analysis of protein extracts from TAM-treated E11.5 whole control and mutant embryos, using anti-RARA, anti-RARG, or anti-GAPDH antibodies. (P) PCR analysis of genomic DNA extracted from TAM-treated E11.5 control and mutant embryos used for protein extraction. This experiment proves efficient excision of the *Rara* and *Rarg* alleles in the whole embryos, as assessed by the absence of L2 alleles in the mutants. The asterisk points to unspecific DNA fragments amplified in all samples. Ao, dorsal aorta; C, cornea; CT, conotruncal ridges; D, dermis; E, epidermis; Go, gonadal ridge; L, lens; M, dorsal mesentery of the hindgut; Po, periocular mesenchyme; R, retina; SV, subcardinal vein. The dotted lines mark off the periphery of the heart outflow tract. White arrowheads indicate nuclei that are still expressing RARG in the mutant tissues. Scale bar (in H), 160 μ m (A and E), 80 μ m (B, C, F, G, I, J, M, and N), and 40 μ m (D, H, K, and L). Photo credits: Norbert B. Ghyselinck and Manuel Mark, IGBMC.

the expression level of *Stra8* in mutant germ cells almost reached the level measured in control germ cells at E13.5 (Fig. 4I). These observations suggested that *Stra8* expression might be delayed in the absence of RARs.

Ablation of RARs at an earlier developmental stage markedly affects embryonic development but not meiosis initiation

When treated by TAM at E10.5, the mutant fetuses displayed, at E14.5, some of the eye defects typically observed in *Rarb*^{-/-}; *Rarg*^{-/-} knock-

out fetuses (fig. S5). However, overall, these mutant fetuses were much less malformed than expected from previous works (16). For instance, the cardiac defects described in *Rara*^{-/-}; *Rarg*^{-/-} knockout fetuses were not observed. To test for the possibility that this discrepancy could be because of the timing of RARs ablation, we treated pregnant females with TAM at E9.5 and analyzed the phenotypes induced in fetuses at E14.5. The mutants generated in this way displayed most of the congenital malformations that are hallmarks of the loss of RARs (Fig. 5). We conclude therefore that deletion of RARs with TAM at E9.5 recapitulates the pathological phenotypes

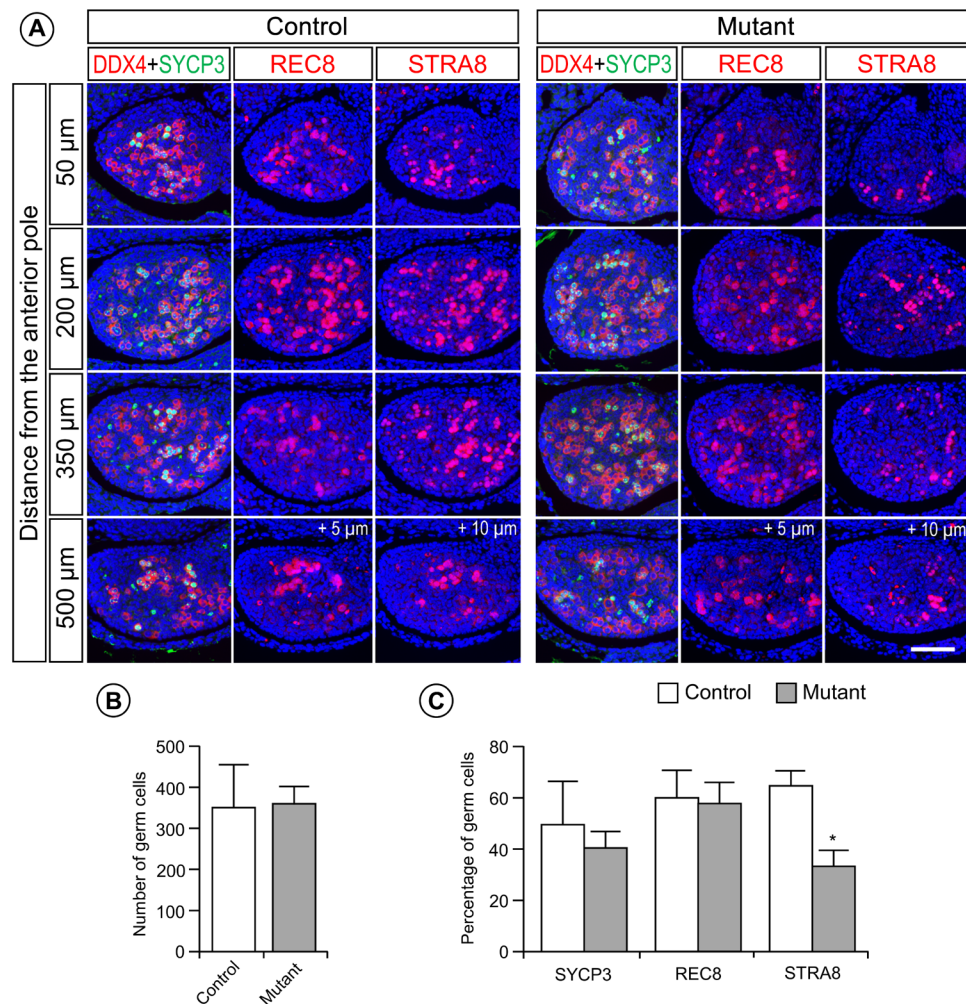


Fig. 3. Markers of meiotic prophase I are robustly expressed at E14.5 in ovaries of mutants lacking RARs. (A) Detection of meiotic cells expressing SYCP3 (green nuclear signal) and REC8 or STRA8 (red nuclear signals) on consecutive, 5- μ m-thick, transverse histological sections at four different levels of the ovaries from control and mutant fetuses, as indicated. DDX4 (red cytoplasmic signal) is present in all germ cells. The positions of histological sections along the anteroposterior axis are indicated in terms of distance from the anterior pole of the ovary (i.e., 50, 200, 350, and 500 μ m). +5 and +10 μ m: The indicated histological sections “REC8” and “STRA8” on each line are, respectively, 5 and 10 μ m apart from the indicated section “DDX4+SYCP3” that was used to establish the total number of germ cells. Nuclei are counterstained with DAPI (blue signal). Scale bar, 60 μ m. (B) Average of the total number of germ cells present at the four different levels of the ovary illustrated in (A) in four control (white bars) and four mutant (gray bars) fetuses at E14.5. (C) Mean percentages of germ cells expressing SYCP3, REC8, and STRA8 in four control (white bars) and four mutant (gray bars) fetuses at E14.5. The asterisk (C) indicates a significant difference ($P < 0.05$). Photo credits: Norbert B. Ghyselinck and Manuel Mark, IGBMC.

observed in the compound knockouts of RARs (i.e., in *Rara*^{-/-};*Rarb*^{-/-}, *Rara*^{-/-};*Rarg*^{-/-}, and *Rarb*^{-/-};*Rarg*^{-/-} fetuses).

Given the role assigned to ATRA in sex determination (17) and PGC proliferation (18), one might have expected that deleting RARs at E9.5 would affect the gonads more markedly than at E10.5. Yet, ovaries formed in mutants and contained normal amounts of germ cells, out of which many of them were meiotic, as indicated by their expression of SYCP3 at E14.5 (fig. S6).

To test for the possibility of a delay in meiosis entry in the absence of RAR (see above), we analyzed at E15.5 control and mutant ovaries of fetuses treated by TAM at E9.5. Virtually, all germ cells had entered meiosis in the mutant ovaries, as attested by the detection of SYCP3 in almost all germ cells (Fig. 6, A and B). Moreover, most of the germ cells showed thread-like segments of synaptonemal complexes positive for SYCP1 and SYCP3, indicating that they were at the zygotene stage (Fig. 6, C and D). In addition, expression of the

mGFP reporter transgene in all germ cells containing such thread-like segments of synaptonemal complexes indicated that these cells had actually experienced cre-mediated gene excision and had therefore lost RAR expression (Fig. 6, E and F). Altogether, our results indicate that RARs are indispensable neither to enter meiosis nor to express STRA8 in germ cells. No increase in apoptosis was evidenced in the mutant ovaries, excluding thereby the possibility that some of the RAR-deficient germ cells experienced cell death (fig. S7, A to C). We conclude that in females, RARs are required neither for gonad differentiation nor for meiosis, up to the zygotene stage.

Oocytes devoid of RARs are functional

As RAR-null fetuses die before birth, it was not possible to analyze their ovaries at late stages. To investigate whether meiosis can proceed beyond the zygotene stage in the absence of RARs, we collected mutant ovaries at E17.5 and grafted them into nude recipient wild-type

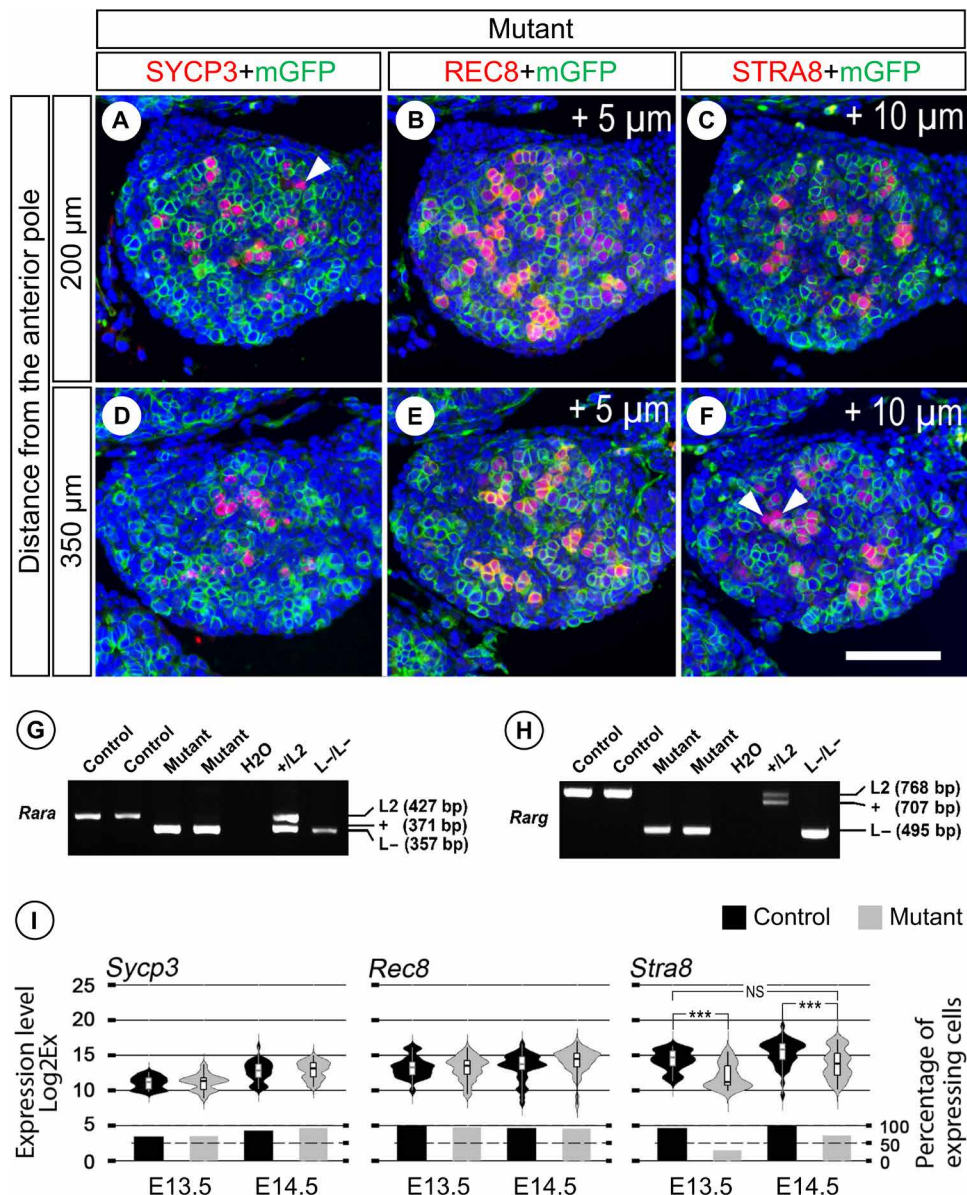


Fig. 4. Evidence that gene excision has actually occurred in meiotic cells 4 days after administration of TAM. (A to F) Detection of the meiotic markers SYCP3, REC8, or STRA8 (red nuclear signals) and of mGFP (green membranous signal) on consecutive, 5- μ m-thick, transverse histological sections at two different levels of the ovary of a mutant fetus at E14.5. Efficient excision of the reporter transgene by *cre/ERT²* is assessed by mGFP expression in virtually all meiotic germ cells. Possible exceptions (i.e., red nuclei without a green contour) are indicated by white arrowheads. The position of histological sections along the anteroposterior axis is indicated on the left side in terms of distance from the anterior pole of the ovary (i.e., 200 and 350 μ m). + 5 and + 10 μ m: The indicated histological sections “REC8+mGFP” and “STRA8+mGFP” on each line are, respectively, 5 and 10 μ m apart from the indicated section “SYCP3+mGFP.” Nuclei are counterstained with DAPI (blue signal). Scale bar (F), 60 μ m. (G and H) PCR analysis of genomic DNA extracted from ovaries of control and mutant fetuses at E13.5, as indicated. (I) RT-qPCR analysis comparing the levels and distributions of mRNAs in single germ cells from control and mutant ovaries at E13.5 and E14.5. The violin plot width and length represent, respectively, the number of cells and the range of expression (Log2Ex). The box-and-whisker plots illustrate medians, ranges, and variabilities of the collected data. The histograms show the percentages of expressing cells in each group. NS, not significantly different; ****P* < 0.001. Photo credits: Norbert B. Ghyselinck and Manuel Mark, IGBMC.

females. When mated with CD1 wild-type males, these females gave birth to pups heterozygous for the *Rara* and *Rarg* excised (L⁻) alleles (Fig. 6H). Control ovaries were also grafted into recipient females, which, as expected, gave birth to pups heterozygous for the *Rara* and *Rarg* floxed (L2) alleles (Fig. 6G). This result indicates that the ovaries of mutants lacking RARs produce functional oocytes (i.e., able to complete meiosis and fertilization) and confirms that the entire meiotic process can take place in the absence of RARs.

Ablation of RARs has no impact on the fetal testis

At about E13.5, when female gonocytes initiate prophase I of meiosis, male gonocytes undergo mitotic arrest in G₀ with all cells having entered the quiescence phase by E16.5 (19). Both ATRA administration at E13.5 and deletion of the gene encoding the ATRA-degrading enzyme CYP26B1 prevent this mitotic arrest and increase apoptosis of male gonocytes (20, 21). In this context, it is interesting to note that the testes of E15.5 mutants lacking all RAR displayed a normal

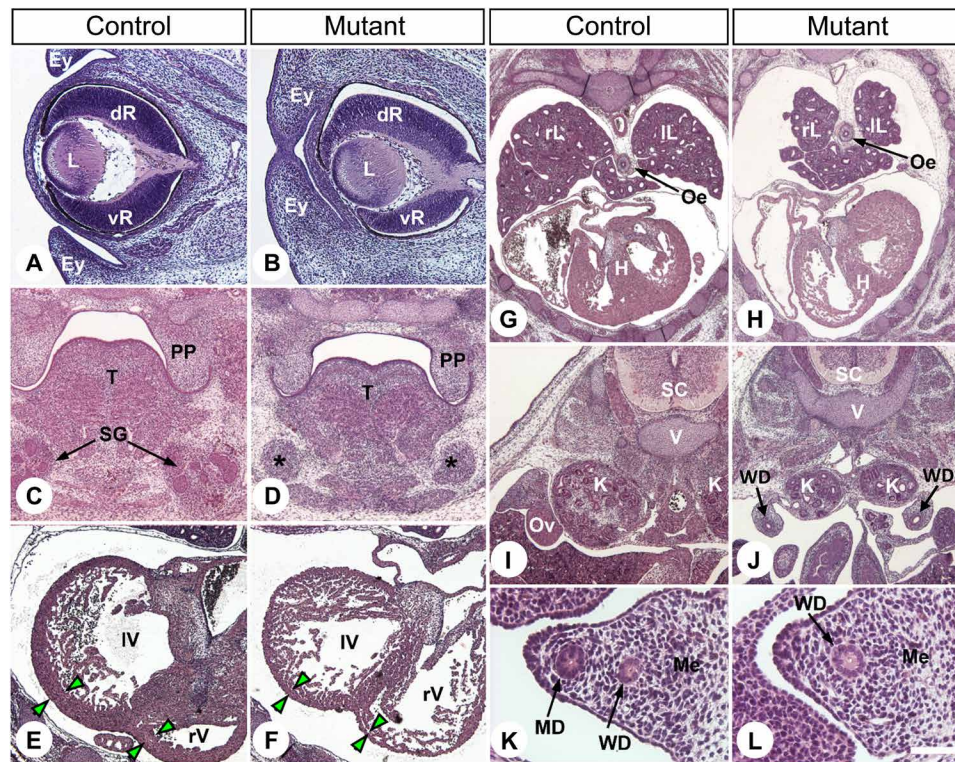


Fig. 5. Mutant fetuses generated upon TAM injection at E9.5 display a spectrum of congenital defects typically observed at E14.5 in compound RAR-knockout mutants. Frontal histological sections at similar levels of E14.5 control and mutant female fetuses. (A and B) In mutants, the ventral portion of the retina (vR) is reduced in size in comparison to the dorsal retina (dR), the lens is rotated ventrally, and the eyelid folds (Ey) are fused together. (C and D) Mutants display mesenchymal condensations indicating the position of the salivary glands [asterisks in (D)], but their epithelial portion [SG in (C)] is absent. (E and F) In mutants, the thickness of the compact layer of the myocardium (green arrowheads) is markedly reduced in both right and left ventricles (rV and IV, respectively). (G and H) Mutants display hypoplasia of the right and left lungs (rL and IL, respectively). (I and J) Mutants have hypoplastic kidneys (K). Note that at this level of the pelvic cavity, the section does not pass through the mutant ovary, which is of normal size and located anteriorly. (K and L) Mutants lack the Müllerian duct [MD in (K)]. Sections were stained with H&E. H, heart; Oe, esophagus; Ov, ovary; PP, palatal process; SG, salivary glands; T, tongue; WD, Wolffian duct. Scale bar (in L), 160 μ m (A and B), 320 μ m (C to F, I, and J), 640 μ m (G and H), and 60 μ m (K and L). Photo credits: Norbert B. Ghyselinck and Manuel Mark, IGBMC.

size and histology, as well as normal, low, amounts of proliferative and apoptotic germ cells (fig. S8). These results imply that RAR signaling is instrumental neither to the survival of fetal male germ cells nor to their exit from the cell cycle.

DISCUSSION

It is widely believed that ATRA synthesized by the mesonephros is an essential paracrine factor diffusing into the ovary to trigger the differentiation of oogonia to oocytes, which then progress into meiosis (8, 22). Nonetheless, germ cells can initiate meiosis in the absence of ALDH1A2, the ATRA-synthesizing enzyme detected in the mesonephros (5). This seemingly contradictory data have been the source of heated and passionate debates (9, 23), but the discovery that the weak ATRA-synthesizing enzyme ALDH1A1 is capable of generating some ATRA in the developing mouse ovary (6) tailored an explanation for the finding that ovarian germ cells remain able to enter meiosis in *Aldh1a2*^{-/-} knockout fetuses (22). We designed the present genetic study to address the question as to whether ATRA-receptors are required for meiosis initiation in the mouse female germ cells.

Our results clearly show that meiotic cells expressing STRA8, REC8, and SYCP3 are present in ovaries lacking RARs. Furthermore, we also show that meiosis proceeds entirely in the absence of

RARs, as functional oocytes are produced from mutant ovaries, when grafted into a recipient mother. These findings suggest that ATRA cannot be the molecule triggering meiosis, except if it acts through a RAR-independent mechanism. Cellular retinoic acid binding protein 1 (CRABP1) is able to mediate such RAR-independent activities of ATRA, notably by activating extracellular signal-regulated kinase 1/2 (ERK1/2)-dependent phosphorylation (24), a pathway involved in meiotic initiation (25). However, the involvement of CRABP1 can be ruled out, since *Crabp1*-null mice are fertile (26, 27), and their ovaries appear fully normal (fig. S7, D and E). In keeping with the notion that ATRA does not trigger meiosis, the report by Chassot and co-workers (accompanying manuscript) shows that simultaneous ablation of all *Aldh1a* genes coding for ATRA-synthesizing enzymes in the ovary does not impair *Stra8* expression and meiosis initiation. This finding echoes the recent observation that both initiation of meiosis and expression of *Stra8* by spermatocytes occur without ATRA (28).

Our results apparently contradict previous observations (8, 9, 22), but several explanations can be proposed to reconcile the discrepancies. First, experiments performed using BMS-204493 (4, 29, 30) and AGN193109 (3, 6, 17) to impair ATRA signaling in fetal ovaries and testes must be interpreted with caution. Actually, these ligands are not RAR antagonists, as they are usually referred to as, but pan-RAR

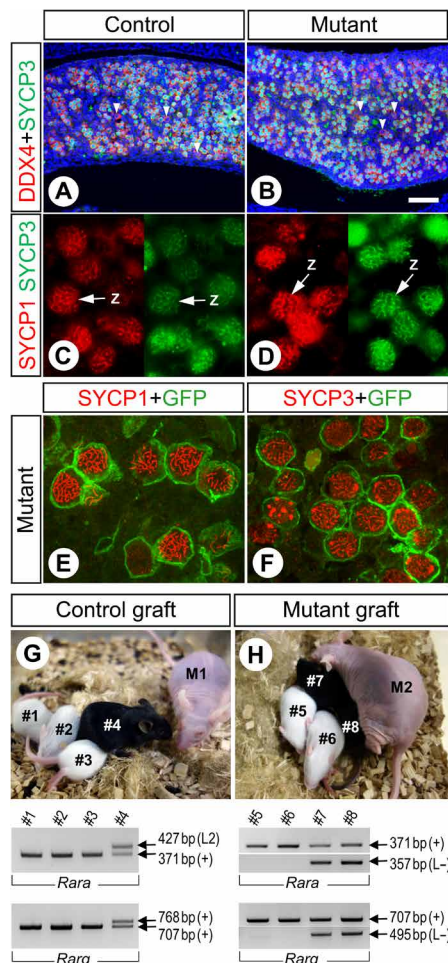


Fig. 6. All germ cells have entered meiosis at E15.5 in ovaries of mutants lacking RARs. (A and B) Detection of germ cells (DDX4 positive, red cytoplasmic signal) expressing SYCP3 (green nuclear signal): In both control (A) and mutant (B) ovaries, almost all germ cells express SYCP3 at high levels; exceptions (i.e., cells expressing SYCP3 at low to undetectable levels) are indicated by white arrowheads. (C and D) High-power magnification views of germ cells immunostained for detection of SYCP1 (red signal) and SYCP3 (green signal): Thread-like structures of SYCP1 and SYCP3 indicate the zygotene stage (Z). (E and F) Detection of SYCP1 or SYCP3 (red nuclear signals) and mGFP (green membranous signal) in the ovary of a mutant fetus also bearing the *mT/mG* reporter transgene. All germ cells that have experienced cre-mediated recombination (mGFP positive) contain thread-like structures of SYCP1 and SYCP3. Nuclei are counterstained with DAPI (blue signal). (G and H) Upper panels: Mice grafted with control (G) or mutant (H) E17.5 ovaries and mated with a CD1 male yielded black/agouti progenies, which were numbered #1 to #8. M1 and M2 are the recipient mothers. Lower panels: PCR analysis of genomic DNA extracted from white and black/agouti progenies as indicated. Scale bar (in B), 60 μ m (A and B) and 10 μ m (C to F). Photo credits: Norbert B. Ghyselinck and Manuel Mark, IGBMC.

inverse agonists, which are capable of repressing RAR basal activity by favoring and stabilizing recruitment of corepressors, even in the absence of an endogenous agonistic ligand such as ATRA (31, 32). As RAR binding sites are present in the *Stra8* promoter on which RARs are actually bound in vivo (5, 33), adding a pan-RAR inverse agonist predictably induces recruitment of NCOR1 and NCOR2 corepressors at the locus, promotes chromatin compaction and thereby *Stra8* extinction, irrespective of the presence of ATRA in the ovary.

The same holds true for the *Rec8* gene, which also contains a RARE (33). The fact that expression of these two genes is artificially shut down upon exposure to a pan-RAR inverse agonist does not mean that their expression is normally controlled by endogenous ATRA. If one assumes that *Rec8* and *Stra8* are actually not regulated by endogenous ATRA, it is logical to find them expressed in germ cells lacking RARs (present study). For the same reason, the fact that AGN193109 abrogates the ectopic expression of *Stra8* in *Cyp26b1*-null mouse testes is not a proof that normal expression of *Stra8* depends on ATRA signaling. Therefore, it cannot be used by Bowles *et al.* (6) as an argument to quash the theory proposed by Kumar *et al.* (5) in 2011 that a molecule distinct from ATRA is involved in the initiation of meiosis. Second, it has been recurrently emphasized that alterations generated by exogenously administered ATRA do not necessarily reflect physiological processes (16, 34). In the case of the gonads, the simple fact that RAR-binding sites are present in *Stra8* and *Rec8* genes can explain their forced expression and initiation of meiosis by supraphysiological concentrations of ATRA added to mouse testes cultured in vitro (3, 4).

Both the number of STRA8-positive cells and the level of *Stra8* expression are lower at E13.5 in RAR-null than in control ovaries. However, this difference diminishes at E14.5, and at E15.5, the proportion of oocytes that are at the late leptotene and zygotene stages is similar in mutant and control ovaries. It is therefore reasonable to propose that RARs participate to the timed expression of *Stra8* in the fetal ovary but are actually not indispensable. Actually, other transcription factors such as MSX1, MSX2 (35), and DMRT1 (36), other signaling pathways such as bone morphogenetic proteins (BMPs) (29, 35) and Activin A (37), as well as the epigenetic status of chromatin (38) appear more important than ATRA for proper *Stra8* expression in the fetal ovary. On top of that, the genetic background may also have some effects on the expression of *Stra8* and on the initiation of meiosis. Actually, *Stra8* knockout males can initiate meiosis in a 129Sv/C57BL6 mixed background (39), but not in a pure C57BLB6 background (40).

Involvement of ATRA in meiosis is commonly interpreted according to the prevailing idea according to which both an MIS, ATRA, and an MPS, the ATRA-degrading enzyme CYP26B1, are required to account for the sex-specific timing of meiotic initiation (8, 9). Since the present work disqualifies ATRA as an MIS, the search for a different molecule should be revived. Alternatively, considering the “MPS-only” hypothesis would reconcile the discrepancies present in the literature (41). According to this scenario, germ cells are programmed to initiate meiosis unless prevented from doing so by an MPS produced in the fetal testis (41). This MPS is CYP26B1 itself or a yet unknown metabolite produced by CYP26B1 (5).

MATERIALS AND METHODS

Mice, treatments, and grafts

Mice were on a mixed C57BL/6 (50%)/129/SvPass (50%) genetic background. They were housed in a licensed animal facility (agreement #C6721837). All experiments were according to Institutional Animal Care and Use Committee guidelines. They were approved by the local ethical committee (Com’Eth, accreditations APAFIS#5638-2016061019045714, APAFIS#5639-201606101910981, and APAFIS#21261-2019062810414395) and were supervised by N.B.G., M.M., and N.V., who are qualified in compliance with the European Community guidelines for laboratory animal care and use (2010/63/UE).

To inactivate *Rar*-coding genes, mice bearing *loxP*-flanked (L2) alleles of *Rara* and *Rarg* (28) and null (L⁻) alleles of *Rarb* (42) were crossed with mice bearing the ubiquitously expressed, TAM-inducible, *cre/ERT²* recombinase-coding *Tg(Ubc-cre/ERT²)* transgene (43). Females homozygous for L2 alleles of *Rara* and *Rarg* and for L⁻ alleles of *Rarb* (i.e., *Rara*^{L2/L2}; *Rarg*^{L2/L2}; *Rarb*^{L-/L-}) were mated with males bearing one copy of the *Tg(Ubc-cre/ERT²)* and homozygous for L2 alleles of *Rara* and *Rarg* and for L⁻ alleles of *Rarb* [i.e., *Tg(Ubc-cre/ERT²)*; *Rara*^{L2/L2}; *Rarg*^{L2/L2}; *Rarb*^{L-/L-}]. Noon of the day of a vaginal plug was taken as 0.5 day embryonic development (E0.5). To activate the *cre/ERT²* recombinase in embryos, one TAM treatment (130 mg/kg body weight) was administered to the pregnant females by oral gavage at E9.5 or at E10.5. TAM (T5648, Sigma-Aldrich) was dissolved in ethanol at a concentration of 100 mg/ml and further diluted in sunflower oil to a concentration of 10 mg/ml. This resulted in embryos or fetuses null for *Rarb*, in which *Rara* and *Rarg* were ablated upon TAM induction when they were bearing *Tg(Ubc-cre/ERT²)* (referred to as mutants), as well as their control littermates when the embryos or fetuses were free of *Tg(Ubc-cre/ERT²)* (referred to as controls). Embryos, fetuses, and females null for *Rarb* display normal ovaries and are totally fertile (42).

To assess for *cre/ERT²*-directed excision, we introduced the *Gt(ROSA26)^{ACTB-tdTomato-EGFP}* reporter transgene (referred to as *mT/mG*), which directs expression of an mGFP in cells that have experienced *cre*-mediated deletion (44), in the *Tg(Ubc-cre/ERT²)*; *Rara*^{L2/L2}; *Rarg*^{L2/L2}; *Rarb*^{L-/L-} genetic background. Embryos and fetuses were collected by caesarean section, and the yolk sacs, tail biopsies, or female gonads were taken for DNA extraction. DNA was genotyped using primers 5'-CAGGGAGGATGCTGTTTGTGA-3', 5'-AACTGCTGCTCTGGGTCTCG-3', and 5'-TACACTAACTACCCCTTGACC-3' to amplify the *Rara* wild-type [+ , 371 base pair (bp) long], the *Rara* L2 allele (427 bp long), and the *Rara* L⁻ (357 bp long) alleles. DNA was genotyped using primers 5'-TGCTTAGCATACTTGAGAAC-3', 5'-ACCGCACGACACGATAGGAC-3', and 5'-GTAGATGCTGGGAATGGAAC-3' to amplify the *Rarg* wild-type (+ , 707 bp long), the *Rarg* L2 (768 bp long), and the *Rarg* L⁻ (495 bp long) alleles. Other genotypes were determined as described (42–44). Wild-type female (*Rara*^{+/+}; *Rarg*^{+/+}; *Rarb*^{+/+}) mated with *Tg(Ubc-cre/ERT²)*; *Rara*^{L2/L2}; *Rarg*^{L2/L2}; *Rarb*^{L-/L-} males and treated with TAM at E10.5 yielded fetuses that were alive and healthy when collected by caesarean delivery at E18.5. This indicates that *cre* on its own has no effect, as previously described (43).

Ovarian transplantation was performed as described (45). Briefly, ovaries were dissected from TAM-treated control (*n* = 6) and mutant (*n* = 4) fetuses at E16.5 and transferred to phosphate-buffered saline (PBS). They were kept at room temperature until transplantation, for a maximum of 2 hours. Recipient females (*n* = 5; nude strain, 8 weeks old) were anesthetized and ovariectomized bilaterally: Through an incision of the ovarian capsule, each ovary was removed at the hilum. One donor fetal ovary was then placed into each of the empty ovarian capsules. The organs were returned into the abdominal cavity, and the wall and skin were sutured. After a 4-week postsurgical recovery, females were caged with fertile CD1 males. One week after delivery, the pups were genotyped.

External morphology, histology, and IHC

Following collection, E11.5 embryos to E15.5 fetuses were fixed overnight in cold 4% (w/v) paraformaldehyde (PFA) in PBS. After removal of the fixative, embryos and fetuses were rapidly rinsed in

PBS and placed in 70% (v/v) ethanol for long-term storage and external morphology evaluation. They were next embedded in paraffin. Consecutive, frontal, 5- μ m-thick sections were made throughout the entire specimens. For histology, sections were stained with hematoxylin and eosin (H&E). For IHC, antigens were retrieved for 1 hour at 95°C either in 10 mM sodium citrate buffer (pH 6.0) or, only in the case of IHC for detection of REC8 and SYCP1, in tris-EDTA (pH 9.0) [10 mM tris base, 1 mM EDTA, and 0.05% (v/v) Tween 20]. Sections were rinsed in PBS and then incubated with appropriate dilutions of the primary antibodies or a mixture of them (e.g., anti-DDX4 and anti-SYCP3; anti-SYCP1 and anti-SYCP3) in PBS containing 0.1% (v/v) Tween 20 (PBST) for 16 hours at 4°C in a humidified chamber. After rinsing in PBST (three times for 3 min each), detection of the bound primary antibodies was achieved for 45 min at 20°C in a humidified chamber using Cy3-conjugated or Alexa Fluor 488-conjugated antibodies, according to the origin of the primary antibody (table S1). Nuclei were counterstained with 4',6-diamidino-2-phenyl-indole (DAPI) diluted at 10 μ g/ml in the mounting medium (Vectashield, Vector). Each experiment was repeated on at least three different fetuses per genotype, age, and stage of TAM treatment.

In situ hybridization

For detection of *Stra8* mRNA, ISH was performed with digoxigenin-labeled probes as previously described (12). For detection of *Rara* mRNA, a commercially available kit was used, according to the manufacturer's instructions (BaseScope Detection Reagent Kit v2-RED, Advanced Cell Diagnostics, 323900). Briefly, deparaffinized sections from PFA-fixed E11.5 embryos were treated with hydrogen peroxide for 10 min, washed, and boiled at 100°C in 1X Target Retrieval Reagent for 10 min. Next, Protease IV was then applied for 15 min at 40°C on dehydrated sections, and then, slides were washed in distilled water. The prewarmed probes (*Rara* and *Ppib* house-keeping gene positive control) were applied on the sections for 2 hours at 40°C. The slides were washed in 1X wash buffer and were subjected to a series of signal amplification (AMP1 to AMP8). Hybridization signals were detected using a chromogenic Fast RED-B/Fast RED-A reagent. The presence of *Rara* and *Ppib* mRNA was identified as red punctate dots. The sections were counterstained for 3 min with 12.5% (v/v) Harris hematoxylin diluted in distilled water.

Western blotting

Protein extracts from whole embryos were prepared in radioimmuno-precipitation assay lysis buffer containing 50 mM tris HCl (pH 7.5), 150 mM NaCl, 0.5% (w/v) sodium deoxycholate, 1% (v/v) NP-40, 0.2% (v/v) sodium dodecyl sulfate (SDS), and protease inhibitors (Sigma-Aldrich, 11873580001). They were resolved by 4 to 20% (w/v) gradient SDS polyacrylamide gel electrophoresis (Expedeon, NXG42012) and transferred to nitrocellulose membranes (Bio-Rad, 1704270) using a standard protocol. The membranes were incubated with anti-RARA or anti-RARG antibodies (table S1) diluted 1:500 and were detected using horseradish peroxidase-coupled goat anti-rabbit antibodies diluted 1:10,000, followed by chemiluminescence using ECL (enhanced chemiluminescence) Western Blotting Substrate (Thermo Fisher Scientific, 32209). To verify the equivalent loading in all the lanes, the membranes were further probed with anti-GAPDH (glyceraldehyde phosphate dehydrogenase) antibodies diluted 1:5000.

Characterization and counts of germ cells

Germ cell counts were performed on pairs of fetuses consisting of one mutant and one of its control littermates, and each experiment was repeated on at least three different fetuses per genotype, age, and stage of TAM treatment. The total number of germ cells in ovaries of control and mutant E14.5 fetuses was quantified using immunostaining for DDX4. Meiotic germ cells were quantified using immunostaining for SYCP3, REC8, and STRA8. A double immunostaining for SYCP1 and SYCP3 was performed to detect germ cells at the zygotene stage. Data were expressed as percentages related to the number of DDX4-positive cells. For apoptosis analysis, more than 400 TRA98-positive cells were counted on transverse histological sections of ovaries, spaced 25 μm apart from each other, from two mutant and two control fetuses at E14.5. In fetal testes, more than 500 TRA98-positive cells were counted on longitudinal histological sections, spaced 25 μm apart from each other, from three mutant and three control fetuses at E15.5. Statistical analysis was done by a two-tailed Student's *t* test, assuming unequal variances after arcsine transformation of the percentages of germ cells expressing the meiotic markers.

Single-cell RNA-seq and RAR expression in fetal germ cells

Mouse urogenital ridges, testes and ovaries collection, single-cell suspension, library preparation, sequencing, data processing, and bioinformatics analysis (normalization, germ cell selection, UMAP projection, pseudotime ordering, and expression curves) were all performed according to the methods described by Mayère *et al.* (13), a manuscript available on bioRxiv (doi: <https://doi.org/10.1101/747279>).

Single-cell RT-qPCR and data processing

Gonads from E13.5 and E14.5 control and mutant fetuses were dissected out in PBS and sexed by their appearance under the microscope. Ovaries (E13.5 controls, $n = 2$; E13.5 mutants, $n = 2$; E14.5 controls, $n = 2$; E14.5 mutants, $n = 3$) were separated from mesonephros using the cutting edge of a 25-gauge needle. Dissociated cells were obtained by incubating the gonads for 15 min in PBS containing 0.5 μM EDTA (46). To allow cell pricking, gonads were then transferred in PBS containing bovine serum albumin (4 mg/ml). Cells were released by puncture of the gonad with 25-gauge needles. This technique generally resulted in a suspension of germ cells, which are recognized as large, refringent cells, with low somatic cell contamination. Cells ($n = 88$ at E13.5 and $n = 132$ at E14.5) were collected individually using pulled Pasteur pipets and transferred as isolated, single cells into microtubes containing 5 μl of cold 1X SuperScript IV VILO Master Mix for two-step RT-qPCR containing 6 units RNasin (Promega) and 0.5% (v/v) NP-40. The microtubes were then stored at -80°C for later processing. Two-step, single-cell gene expression analysis was achieved on the BioMark HD system (Fluidigm) using SsoFast EvaGreen Supermix with low ROX (Bio-Rad Laboratories) according to the manufacturer's instructions. The set of primers used for qPCR are listed (table S2). Cycle thresholds (Ct) were recovered and analyzed by the Fluidigm Real-Time PCR Analysis software, using the linear (derivative) baseline correction method and the auto (global) Ct threshold method. Limit of detection (LOD) was set to a Ct of 28. The quality threshold was set to 0.65. Ct for qPCRs that failed the quality threshold [melting curves with deviating T_m temperatures] were converted to 28. The Ct values were then exported to Excel and converted to expression levels using the equation $\text{Log Ex} = \text{Ct}[\text{LOD}] - \text{Ct}[\text{Assay}]$. The expressions

of *Actb* and *Tbp* housekeeping genes were measured to determine which sample actually contained a cell. Cells that fail to amplify systematically all the tested genes or to express germ cell markers (*Dazl*, *Ddx4*, and *Kit*) were excluded from further analysis. The percentages of cells excluded were 23% at E13.5 and 34% at E14.5, respectively. This can be explained by the greater difficulty to isolate and collect germ cells at E14.5, compared with E13.5. The final analysis was done using $n = 68$ individual cells at E13.5 ($n = 25$ controls and $n = 43$ mutants) and $n = 87$ individual cells at E14.5 ($n = 40$ controls and $n = 47$ mutants). Results were not normalized relative to housekeeping genes, as their expression did not differ between control and mutant cells. Percentages of cells expressing a gene of interest are represented as histograms, and expression levels are represented as violin and box plot using R Studio software. To assess for variation of expression, we first verified that the variances were equal or not (*F* test). Then, an appropriate two-tailed Student's *t* test was performed on the Log2Ex values, using Excel software.

SUPPLEMENTARY MATERIALS

Supplementary material for this article is available at <http://advances.sciencemag.org/cgi/content/full/6/21/eaaz1139/DC1>

[View/request a protocol for this paper from Bio-protocol.](#)

REFERENCES AND NOTES

1. A. McLaren, Germ cells and germ cell sex. *Philos. Trans. R. Soc. Lond. B Biol. Sci.* **350**, 229–233 (1995).
2. A. G. Byskov, L. Saxén, Induction of meiosis in fetal mouse testis in vitro. *Dev. Biol.* **52**, 193–200 (1976).
3. J. Bowles, D. Knight, C. Smith, D. Wilhelm, J. Richman, S. Mamiya, K. Yashiro, K. Chawengsaksohak, M. J. Wilson, J. Rossant, H. Hamada, P. Koopman, Retinoid signaling determines germ cell fate in mice. *Science* **312**, 596–600 (2006).
4. J. Koubova, D. B. Menke, Q. Zhou, B. Capel, M. D. Griswold, D. C. Page, Retinoic acid regulates sex-specific timing of meiotic initiation in mice. *Proc. Natl. Acad. Sci. U.S.A.* **103**, 2474–2479 (2006).
5. S. Kumar, C. Chatzi, T. Brade, T. J. Cunningham, X. Zhao, G. Duyster, Sex-specific timing of meiotic initiation is regulated by Cyp26b1 independent of retinoic acid signalling. *Nat. Commun.* **2**, 151 (2011).
6. J. Bowles, C. W. Feng, K. Miles, J. Ineson, C. Spiller, P. Koopman, ALDH1A1 provides a source of meiosis-inducing retinoic acid in mouse fetal ovaries. *Nat. Commun.* **7**, 10845 (2016).
7. Z. Al Tanoury, A. Piskunov, C. Rochette-Egly, Vitamin A and retinoid signaling: Genomic and nongenomic effects. *J. Lipid Res.* **54**, 1761–1775 (2013).
8. J. Bowles, P. Koopman, Retinoic acid, meiosis and germ cell fate in mammals. *Development* **134**, 3401–3411 (2007).
9. M. D. Griswold, C. A. Hogarth, J. Bowles, P. Koopman, Initiating meiosis: The case for retinoic acid. *Biol. Reprod.* **86**, 35 (2012).
10. J. M. Clark, E. M. Eddy, Fine structural observations on the origin and associations of primordial germ cells of the mouse. *Dev. Biol.* **47**, 136–155 (1975).
11. D. B. Menke, J. Koubova, D. C. Page, Sexual differentiation of germ cells in XX mouse gonads occurs in an anterior-to-posterior wave. *Dev. Biol.* **262**, 303–312 (2003).
12. N. Vernet, C. Dennefeld, C. Rochette-Egly, M. Oulad-Abdelghani, P. Chambon, N. B. Ghyselinck, M. Mark, Retinoic acid metabolism and signaling pathways in the adult and developing mouse testis. *Endocrinology* **147**, 96–110 (2006).
13. C. Mayère, Y. Neirijnck, P. Sararols, I. Stévant, F. Kühne, A. A. Chassot, M.-C. Chaboissier, E. T. Dermitzakis, S. Nef, Single-cell transcriptomic reveals temporal dynamics of critical regulators of germ cell fate during mouse sex determination. *bioRxiv*, 747279 (2019).
14. O. Wendling, N. B. Ghyselinck, P. Chambon, M. Mark, Roles of retinoic acid receptors in early embryonic morphogenesis and hindbrain patterning. *Development* **128**, 2031–2038 (2001).
15. A. E. Baltus, D. B. Menke, Y. C. Hu, M. L. Goodheart, A. E. Carpenter, D. G. de Rooij, D. C. Page, In germ cells of mouse embryonic ovaries, the decision to enter meiosis precedes premeiotic DNA replication. *Nat. Genet.* **38**, 1430–1434 (2006).
16. M. Mark, N. B. Ghyselinck, P. Chambon, Function of retinoid nuclear receptors: Lessons from genetic and pharmacological dissections of the retinoic acid signaling pathway during mouse embryogenesis. *Annu. Rev. Pharmacol. Toxicol.* **46**, 451–480 (2006).

17. J. Bowles, C. W. Feng, J. Ineson, K. Miles, C. M. Spiller, V. R. Harley, A. H. Sinclair, P. Koopman, Retinoic acid antagonizes testis development in mice. *Cell Rep.* **24**, 1330–1341 (2018).
18. U. Koshimizu, M. Watanabe, N. Nakatsuji, Retinoic acid is a potent growth activator of mouse primordial germ cells in vitro. *Dev. Biol.* **168**, 683–685 (1995).
19. R. P. Vergouwen, S. G. Jacobs, R. Huiskamp, J. A. Davids, D. G. de Rooij, Proliferative activity of gonocytes, Sertoli cells and interstitial cells during testicular development in mice. *J. Reprod. Fertil.* **93**, 233–243 (1991).
20. E. Trautmann, M. J. Guerquin, C. Duquenne, J. B. Lahaye, R. Habert, G. Livera, Retinoic acid prevents germ cell mitotic arrest in mouse fetal testes. *Cell Cycle* **7**, 656–664 (2008).
21. G. MacLean, H. Li, D. Metzger, P. Chambon, M. Petkovich, Apoptotic extinction of germ cells in testes of *Cyp26b1* knockout mice. *Endocrinology* **148**, 4560–4567 (2007).
22. C. Spiller, J. Bowles, Sexually dimorphic germ cell identity in mammals. *Curr. Top. Dev. Biol.* **134**, 253–288 (2019).
23. S. Kumar, T. J. Cunningham, G. Dueter, Resolving molecular events in the regulation of meiosis in male and female germ cells. *Sci. Signal.* **6**, pe25 (2013).
24. S. D. Persaud, S. W. Park, M. Ishigami-Yuasa, N. Koyano-Nakagawa, H. Kagechika, L.-N. Wei, All trans-retinoic acid analogs promote cancer cell apoptosis through non-genomic Crabp1 mediating ERK1/2 phosphorylation. *Sci. Rep.* **6**, 22396 (2016).
25. S.-M. Kim, T. Yokoyama, D. Ng, F. Ulu, Y. Yamazaki, Retinoic acid-stimulated ERK1/2 pathway regulates meiotic initiation in cultured fetal germ cells. *PLoS One* **14**, e0224628 (2019).
26. D. R. de Bruijn, F. Oerlemans, W. Hendriks, E. Baats, R. Ploemacher, B. Wieringa, A. Geurts van Kessel, Normal development, growth and reproduction in cellular retinoic acid binding protein-I (CRABPI) null mutant mice. *Differentiation* **58**, 141–148 (1994).
27. P. Gorry, T. Lufkin, A. Dierich, C. Rochette-Egly, D. Décimo, P. Dollé, M. Mark, B. Durand, P. Chambon, The cellular retinoic acid binding protein I is dispensable. *Proc. Natl. Acad. Sci. U.S.A.* **91**, 9032–9036 (1994).
28. M. Teletin, N. Vernet, J. Yu, M. Klopfenstein, J. W. Jones, B. Féret, M. A. Kane, N. B. Ghyselinck, M. Mark, Two functionally redundant sources of retinoic acid secure spermatogonia differentiation in the seminiferous epithelium. *Development* **146**, dev170225 (2019).
29. H. Miyauchi, H. Ohta, S. Nagaoka, F. Nakaki, K. Sasaki, K. Hayashi, Y. Yabuta, T. Nakamura, T. Yamamoto, M. Saitou, Bone morphogenetic protein and retinoic acid synergistically specify female germ-cell fate in mice. *EMBO J.* **36**, 3100–3119 (2017).
30. J. Koubova, Y. C. Hu, T. Bhattacharyya, Y. Q. Soh, M. E. Gill, M. L. Goodheart, C. A. Hogarth, M. D. Griswold, D. C. Page, Retinoic acid activates two pathways required for meiosis in mice. *PLoS Genet.* **10**, e1004541 (2014).
31. P. Germain, C. Gaudon, V. Pogenberg, S. Sanglier, A. Van Dorsselaer, C. A. Royer, M. A. Lazar, W. Bourguet, H. Gronemeyer, Differential action on coregulator interaction defines inverse retinoid agonists and neutral antagonists. *Chem. Biol.* **16**, 479–489 (2009).
32. E. S. Klein, M. E. Pino, A. T. Johnson, P. J. Davies, S. Nagpal, S. M. Thacher, G. Krasinski, R. A. Chandraratna, Identification and functional separation of retinoic acid receptor neutral antagonists and inverse agonists. *J. Biol. Chem.* **271**, 22692–22696 (1996).
33. A. Chatagnon, P. Veber, V. Morin, J. Bedo, G. Triqueneaux, M. Sémon, V. Laudet, F. d'Alché-Buc, G. Benoit, RAR/RXR binding dynamics distinguish pluripotency from differentiation associated cis-regulatory elements. *Nucleic Acids Res.* **43**, 4833–4854 (2015).
34. T. J. Cunningham, G. Dueter, Mechanisms of retinoic acid signalling and its roles in organ and limb development. *Nat. Rev. Mol. Cell Biol.* **16**, 110–123 (2015).
35. R. Le Bouffant, B. Souquet, N. Duval, C. Duquenne, R. Hervé, N. Frydman, B. Robert, R. Habert, G. Livera, *Msx1* and *Msx2* promote meiosis initiation. *Development* **138**, 5393–5402 (2011).
36. A. D. Krentz, M. W. Murphy, A. L. Sarver, M. D. Griswold, V. J. Bardwell, D. Zarkower, DMRT1 promotes oogenesis by transcriptional activation of *Stra8* in the mammalian fetal ovary. *Dev. Biol.* **356**, 63–70 (2011).
37. G.-J. Liang, X.-F. Zhang, J.-J. Wang, Y.-C. Sun, X.-F. Sun, S.-F. Cheng, L. Li, M. De Felici, W. Shen, Activin A accelerates the progression of fetal oocytes throughout meiosis and early oogenesis in the mouse. *Stem Cells Dev.* **24**, 2455–2465 (2015).
38. N. Wang, J. L. Tilly, Epigenetic status determines germ cell meiotic commitment in embryonic and postnatal mammalian gonads. *Cell Cycle* **9**, 339–349 (2010).
39. M. Mark, H. Jacobs, M. Oulad-Abdelghani, C. Dennefeld, B. Féret, N. Vernet, C.-A. Codreanu, P. Chambon, N. B. Ghyselinck, *STRa8*-deficient spermatocytes initiate, but fail to complete, meiosis and undergo premature chromosome condensation. *J. Cell Sci.* **121**, 3233–3242 (2008).
40. E. L. Anderson, A. E. Baltus, H. L. Roepers-Gajadien, T. J. Hassold, D. G. de Rooij, A. M. van Pelt, D. C. Page, *Stra8* and its inducer, retinoic acid, regulate meiotic initiation in both spermatogenesis and oogenesis in mice. *Proc. Natl. Acad. Sci. U.S.A.* **105**, 14976–14980 (2008).
41. A. Kocer, J. Reichmann, D. Best, I. R. Adams, Germ cell sex determination in mammals. *Mol. Hum. Reprod.* **15**, 205–213 (2009).
42. B. Chapellier, M. Mark, J. Bastien, A. Dierich, M. LeMeur, P. Chambon, N. B. Ghyselinck, A conditional floxed (*loxP*-flanked) allele for the retinoic acid receptor beta (RAR β) gene. *Genesis* **32**, 91–94 (2002).
43. Y. Ruzankina, C. Pinzon-Guzman, A. Asare, T. Ong, L. Pontano, G. Cotsarelis, V. P. Zediak, M. Velez, A. Bhandoola, E. J. Brown, Deletion of the developmentally essential gene *ATR* in adult mice leads to age-related phenotypes and stem cell loss. *Cell Stem Cell* **1**, 113–126 (2007).
44. M. D. Muzumdar, B. Tasic, K. Miyamichi, L. Li, L. Luo, A global double-fluorescent Cre reporter mouse. *Genesis* **45**, 593–605 (2007).
45. A. Marmolejo-Valencia, Y. Nishioka, N. Moreno-Mendoza, H. Merchant-Larios, Fertility of Y^{TIR}.B6 sex-reversal females with XX orthotopic ovarian transplants. *Biol. Reprod.* **61**, 1426–1430 (1999).
46. M. De Felici, A. McLaren, Isolation of mouse primordial germ cells. *Exp. Cell Res.* **142**, 476–482 (1982).
47. M. A. Carmell, G. A. Dokshin, H. Skaletsky, Y.-C. Hu, J. C. van Wolfswinkel, K. J. Igarashi, D. W. Bellott, M. Nefedov, P. W. Reddien, G. C. Enders, V. N. Uversky, C. C. Mello, D. C. Page, A widely employed germ cell marker is an ancient disordered protein with reproductive functions in diverse eukaryotes. *eLife* **5**, e19993 (2016).
48. H. E. Abud, J. K. Heath, Detecting apoptosis during the formation of polarized intestinal epithelium in organ culture. *Cell Death Differ.* **11**, 788–789 (2004).
49. M. P. Gaub, C. Rochette-Egly, Y. Lutz, S. Ali, H. Matthes, I. Scheuer, P. Chambon, Immunodetection of multiple species of retinoic acid receptor α : Evidence for phosphorylation. *Exp. Cell Res.* **201**, 335–346 (1992).

Acknowledgments: We thank A. Chassot, M.-C. Chaboissier, and E. Pailhoux for the discussions, advices, and critical reading of the manuscript. We also thank C. Thibault-Carpentier from the Genomeast platform for input (<http://genomeast.igbmc.fr/>). The imaging was supported by the Imaging Center of IGBMC (<http://ici.igbmc.fr/>) with E. Grandgirard. **Funding:** This work was supported by grants from CNRS, INSERM, UNISTRA, and Agence Nationale pour la Recherche (ANR-13-BSV6-0003 and ANR-13-BSV2-0017), as well as from EU (FP7-PEOPLE-IEF-2012-331687). It was also supported in part by the grant ANR-10-LABX-0030-INRT, a French State fund managed by the ANR under the frame programme Investissements d'Avenir labeled ANR-10-IDEX-0002-02. **Author contributions:** N.V., S.N., M.M., and N.B.G. designed the study, analyzed the data, and wrote the paper. N.V., D.C., C.M., B.F., M.K., W.M., V.A., M.T., S.S.-C., and M.M. performed the experiments, analyzed the data, and discussed the results. S.N. and M.T. additionally commented on the manuscript. **Competing interests:** The authors declare that they have no competing interests. **Data and materials availability:** All data needed to evaluate the conclusions in the paper are present in the paper and/or the Supplementary Materials. Additional data related to this paper may be requested from the authors.

Submitted 14 August 2019

Accepted 13 March 2020

Published 22 May 2020

10.1126/sciadv.aaz1139

Citation: N. Vernet, D. Condrea, C. Mayere, B. Féret, M. Klopfenstein, W. Magnant, V. Alunni, M. Teletin, S. Souali-Crespo, S. Nef, M. Mark, N. B. Ghyselinck, Meiosis occurs normally in the fetal ovary of mice lacking all retinoic acid receptors. *Sci. Adv.* **6**, eaaz1139 (2020).